Wireless video streaming over integrated 3G and WLAN networks

Ivan Lee*

School of Computer and Information Science,
University of South Australia,
Mawson Lakes, SA 5095, Australia
E-mail: ivanlee@ieee.org
*Corresponding author

Ling Guan

Department of Electrical and Computer Engineering,
Ryerson University,
Toronto, Ontario M5B-2K3, Canada
E-mail: lguan@ee.ryerson.ca

Abstract: Media streaming is a popular application demanding high data rates and hard delay constraints. These requirements raise great challenges in the wireless environment, where signal fading, noise interference and network congestion introduce data losses or corruptions. Today, the availability of the Third Generation (3G) wireless system and the Wireless Local Area Network (WLAN) provides a broader bandwidth to cater for multimedia application. Different characteristics of 3G and WLAN networks result in different attributes in video streaming applications. In this paper, we propose a collaborative scheme across 3G and WLAN networks for video streaming, using layered video coding and Unequal Error Protection (UEP) to improve the perceived video quality.

Keywords: wireless networking; video streaming; layered video coding.

Reference to this paper should be made as follows: Lee, I. and Guan, L. (2007) 'Wireless video streaming over integrated 3G and WLAN networks', *Int. J. Wireless and Mobile Computing*, Vol. 2, No. 4, pp.314–323.

Biographical notes: Ivan Lee received his BE, MCom, MER and PhD degrees from the University of Sydney. He was a Software Engineer at Cisco Systems from 1998 to 2001), a software Team Leader at Remotek Corporation between 2003 and 2004) and an Assistant Professor at Ryerson University between 2005 and 2007). He is now a Senior Lecturer at the University of South Australia. He presently serves on the Editorial Board of IEEE Communications Surveys and Tutorials, and he is an Associate Editor of *Hindawi International Journal of Digital Multimedia Broadcasting*. His research interests include multimedia signal processing and multimedia communication.

Ling Guan is a Professor and Tier I Canada Research Chair in Multimedia at Ryerson University. He received a Masters degree in Systems Design Engineering from the University of Waterloo and a PhD in Electrical Engineering from the University of British Columbia. He has authored/co-authored more than 250 scientific publications in image, video and multimedia processing. He served/serves on the Editorial Board of several *IEEE Transactions/Magazines*, and Chaired the *2007 IEEE International Conference on Multimedia and Expo in Toronto*. He is the recipient of 2005 IEEE CSVT Transactions Best Paper Award.

1 Introduction

Video streaming applications demand a real-time data transmission to fulfil the playback-while-downloading behaviour, in contrast to the conventional display- or process-after-downloading behaviours such as common HTTP services or Multimedia Messaging Services (MMS) (Wu et al., 2001a–c). For wireless video streaming, additional challenges emerge due to factors such as latency, fading and interference (Wu et al., 2001a–c).

Studies for the VBR video transmission over the wireless channel has been investigated by Stockhammer et al. (2004).

In Stockhammer et al. (2003), examined H.264 transmission over the wireless channel, and the performance of layered coding has been investigated by Yang et al. (2004). Multiple Description Coding (MDC) technique has been observed under the wireless ad hoc network by Mao et al. (2003).

To address the issues on signal fading and noise interference, Unequal Error Protection (UEP) was proposed by Zhang and Xu (1999). Stockhammer et al. (2002) introduced a feedback strategy for error resilience under the wireless environment. In Karim et al. (2003), summarises the techniques for loss frame recovery.

In practice, a 3G system such as CDMA-1X has the throughput at around 60–100 kbps. A Wireless Local Area Network (WLAN) system such as 802.11a/g has the throughput of up to 54 Mbps. Another major difference between 3G and WLAN systems is the coverage range and the readiness in practice. Typically, the 3G service coverage for each base station is 1–5 miles, while a WLAN AP serves up to 300 feet. As illustrated in Figure 1, one 3G network can overlap with multiple WLAN networks. Each cellular network is centred with a base-station whereas each WLAN hotspot network is centred with a WLAN AP. Today, the 3G cellular network is more readily established than the WLAN hotspots, and much better network coverage with the 3G network than the WLAN network is expected.

Figure 1 Illustration on 3G and WLAN networks

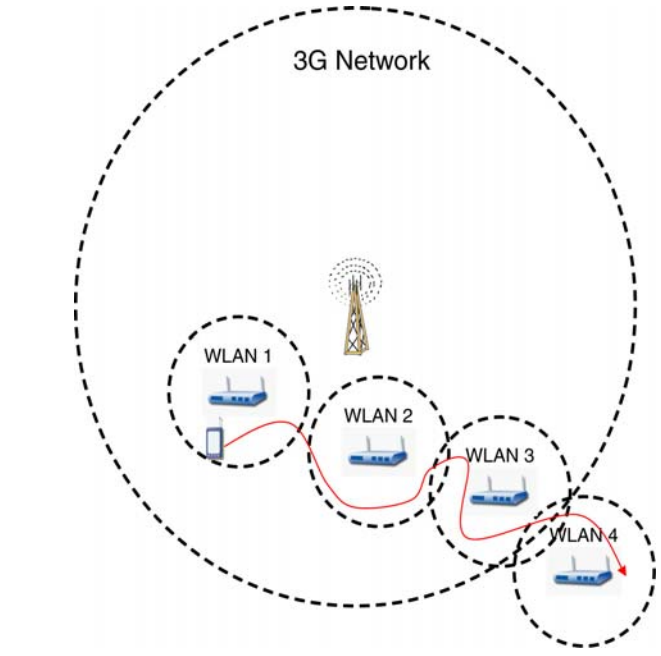

This paper proposes a video streaming infrastructure via an integrated 3G cellular network and the WLAN hotspot network, utilising the different signal coverage range and bandwidth capabilities between the two wireless networks. Advanced layered video coding techniques using Progressive Fine Granularity Scalable (PFGS) with UEP are adopted. To reconstruct loss frame caused by drifting errors, this paper also proposes a temporal domain super-resolution technique using cubic spline interpolation. Investigations on the effectiveness of the buffer size of the end-user device are also analysed in this paper.

For the simulation, this paper addresses the handover behaviour observed in most modern communication systems, and a three-state Markov chain is introduced to represent the good, bad and handover states. The performance of the proposed system is evaluated according to the reconstructed video qualities.

2 Integrated 3G and WLAN video streaming system

The readily established 3G network and the high bandwidth WLAN hotspot network make good complementary counterparts for video streaming applications. To benefit from both networks for video streaming applications, we propose an integrated approach by making the client device capable of establishing connections to 3G and WLAN networks simultaneously.

As illustrated in Figure 2, the video server is located in the IP network. There are two independent paths to transmit the video content to the 3G/WLAN client device: via WLAN AP, or via the 3G network with Gateway GPRS Support Node (GGSN), Serving GPRS Support Node (SGSN), Radio Network Controller (RNC) and Node B. The integrated 3G/WLAN infrastructure proposed in this paper streams the high priority data within the 3G network and the lower priority data within the WLAN network.

Figure 2 Wireless video streaming with integrated 3G/WLAN network

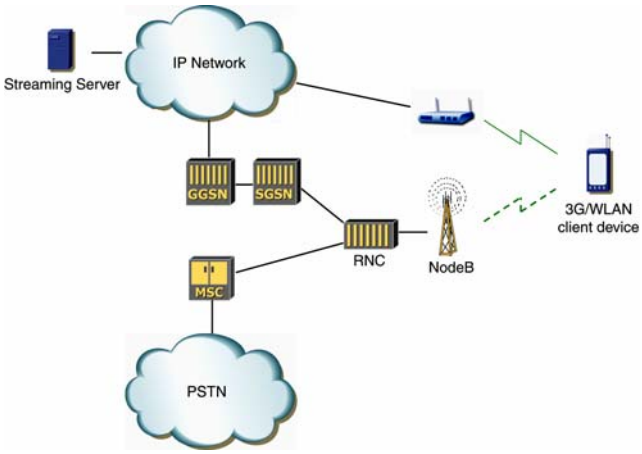

A layered video coder splits a digital video signal into a number of cumulative layers such that a higher quality video can be reconstructed with more layers used in the decoding process. PFGS (Wu et al., 2001a–c) is an advanced layered coding technique proposed for the H.264 standard (Wiegand et al., 2003). In comparison to FGS proposed by Li (2001), PFGS provides higher coding efficiency by using high quality reference frames for enhancement layer coding. In this paper, PFGS with UEP is applied, as shown in the block diagram in Figure 3. Baseline profile of H.264

Figure 3 Block diagram for the video encoder

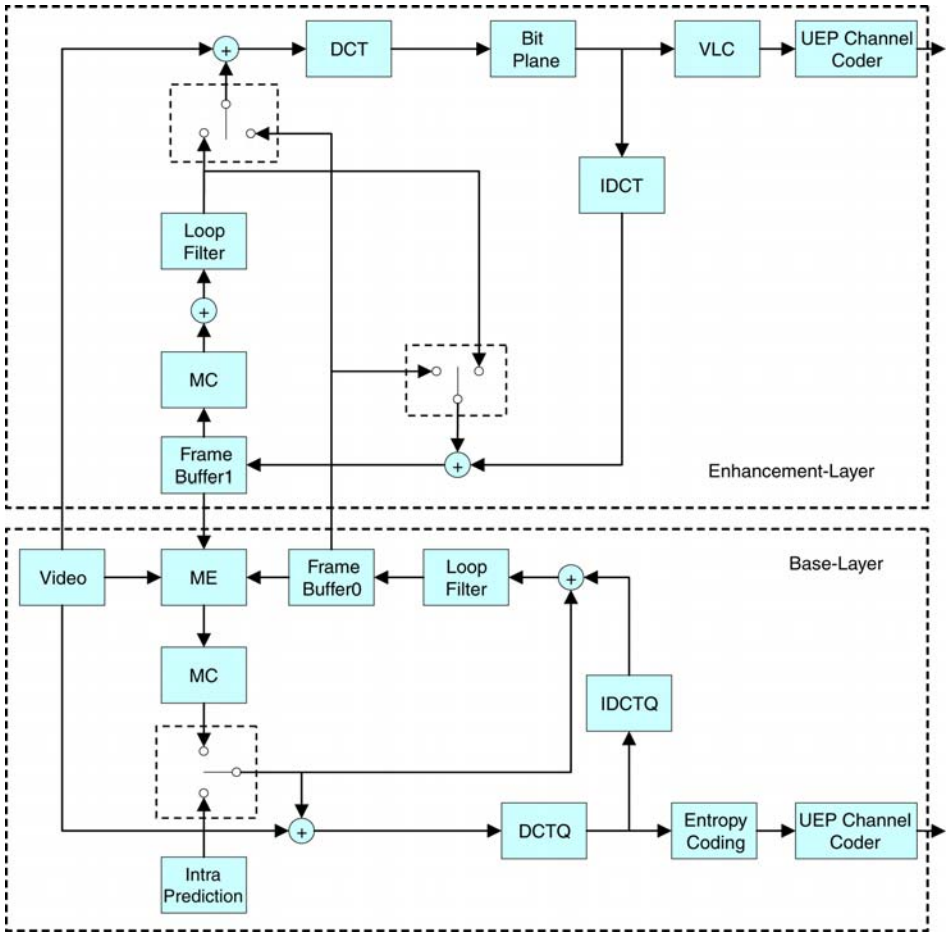

(Ostermann et al., 2004) is applied in this paper, using video bitstream with intra (*I*) and predicted (*P*) frames.

In terms of signal coverage, 3G network is more readily developed than WLAN hotspot network. On the other hand, WLAN possesses higher bandwidth than 3G network. To utilise the benefits from both networks, base layer video (highly prioritised data) will be transmitted over the 3G network, while the enhancement layer video (high bandwidth requirement) will be transmitted over the WLAN hotspot network.

The proposed system is simulated based on a Markov chain. A Markov chain is a discrete-time stochastic process with the Markov property: the state at the current time is decided by only the immediately preceding one and is not influenced by the state at any previous time. In formal terms, the Markov chain follows:

$$P\left(x_{t+1}\middle|x_0,x_1,x_2,\ldots,x_t\right)=P\left(x_{t+1}\middle|x_t\right) \tag{1}$$

A popular simulation model for traffic losses in the data transmission is the Gilbert Model (Yee and Weldon, 1995). Gilbert model is a two-state Markov chain, with a Good state indicating a successful data transmission and a Bad state indicating a data loss. The model reflects the environment where the errors occur in clusters or bursts with relatively long error-free gaps between them.

In this paper, we extend the Gilbert model to a three-state Markov chain model, to represent Good (S_0), Bad (S_1) and Handover (S_2) states. Simply the model, S_2 will only originate from or terminate to S_1, with the assumption that before and after the handover, the client device is moving at the edge of the networks which typically has weak signals or high interferences. Thus, the handover action is assumed to be accompanied with and therefore evolved from the Bad state. The state transitions are shown in Figure 4 with its transition probability matrix summarised in Equation (2).

$$P=\begin{bmatrix} P_{00} & P_{10} & 0 \\ P_{01} & P_{11} & P_{21} \\ 0 & P_{12} & P_{22} \end{bmatrix} \tag{2}$$

Let P denote the steady state probabilities and $P = [P_{S0}P_{S1}P_{S2}]^T$, where P_{Sn} is the steady state probability at state n. P can be expressed as Equation (3). Details of the steady state analysis can be found in Appendix.

$$\begin{bmatrix} P_{S0} \\ P_{S1} \\ P_{S2} \end{bmatrix}=\frac{1}{P_{01}P_{12}+P_{01}P_{21}+P_{10}P_{21}}\begin{bmatrix} P_{10} & P_{21} \\ P_{01} & P_{21} \\ P_{01} & P_{12} \end{bmatrix} \tag{3}$$

The different transmission characteristics of the 3G cellular network and the WLAN hotspot network are reflected in the probability matrix.

Figure 4 Three-state Markov chain model

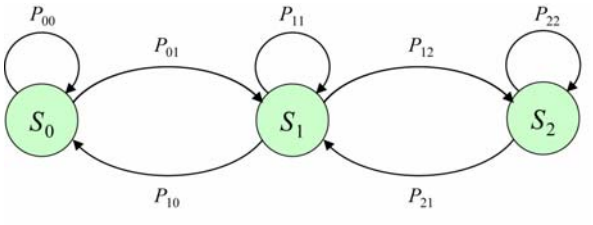

2.1 3G cellular network

The wide availability of 3G network results in lower P_{01} and higher P_{10} relative to WLAN. While the coverage range in a single cell is much larger, the probability of entering the handover state is low, hence reducing P_{12}. In most areas, a 3G network operates with soft-handover to reduce the data loss, which in term increases P_{21}. Reducing P_{12} and increasing P_{21} reflects higher probability for staying at or returning to the Good state.

2.2 WLAN network

Most observable differences of the WLAN hotspot network from the 3G network is the higher probability of moving to the boundary of the cell to start the handover, thus resulting in higher P_{12} and P_{22}. As explained previously, a WLAN hotspot network in general yields higher P_{01}, lower P_{10} and lower P_{21}.

3 Error recovery

3.1 Network adaptive UEP

To address different priority levels associated with the layered video coding, a UEP scheme is deployed. In this project, we choose Turbo code as the channel coding technique to protect different layers of the video stream. Turbo code consists of two concatenated recursive convolutional encoders fed by interleaved versions of the information bits (Berrou et al., 1993), and it is also known as the parallel concatenated convolutional codes. In this project, an additional parity-check mechanism is also included, to identify whether or not the bitstream was successfully recovered from channel codec. Since the corruption of the enhancement layer may introduce a severe visual quality distortion, the layer will be discarded if it is not successfully decoded.

3.2 Buffering for multipath latency and loss recovery with cubic spline interpolation

Latencies in the integrated 3G/WLAN streaming system may lead to synchronisation issues. This is mostly due to multipath delays over two independent networks. In layered video coding, the lower layers are required to decode the upper layers. Failing to receive the lower layers within the real-time constraint will result in the synchronisation problem, which can be reduced by providing a memory buffer on the end-user device. The buffering technique can help improving the video quality caused by multipath latency, with a cost of device memory and the delay to decode the bitstream.

As described previously, PFGS video coding based on baseline profile is used. The video stream consists of intra-frames (*I*) and predicted-frames (*P*), as shown in Figure 5. Predicted frame are constructed based on the inter-frame motion compensation, and is therefore relying on the successful transmission of the previous frames. The interval between the current and the subsequent *I*-frames are referred as *I*-frame interval, denoted by.

Figure 5 Video bitstream

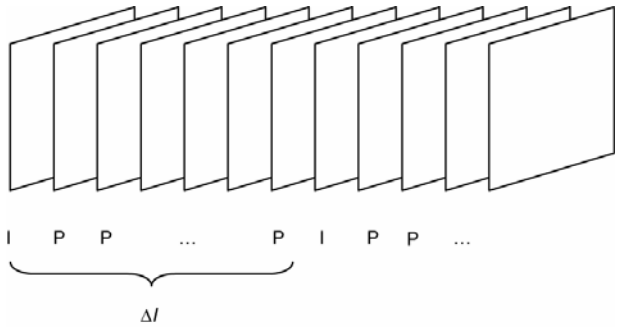

In a motion-compensation-based video codec, a video frame corruption will be propagated to the subsequent video frames, which is known as the drifting error. In general, a larger ΔI leads to a higher probability of drifting error. This can be illustrated in the three-state Markov model: the video frames are dropped in both the Bad and the Handover state, and the overall dropping probability, P_{drop}, can be derived from (3)

$$P_{\text{drop}} = \frac{P_{01}\left(P_{12}+P_{21}\right)}{P_{01}P_{12}+P_{01}P_{21}+P_{10}P_{21}} \tag{4}$$

To recover the loss frames, resampling technique using interpolation is examined in this work. Cubic spline extrapolation and interpolation techniques are selected in this work for its effectiveness and computational efficiency (Lehmann et al., 1999).

Because of the drifting error, the loss occuring at the Bad or Handover state will result in a sequence of frame drop until the arrival of the subsequent *I*-frame. Two approaches can be taken to recover the lost frames.

3.2.1 Uni-directional extrapolation

This approach buffers video frames prior to the frame loss, and performs the extrapolation based on the buffered frames.

3.2.2 Bi-directional interpolation

This approach reconstructs the video frames according to the frames both before and after the lost frames.

Experiments on both approaches are evaluated in the following section. Bi-directional interpolation achieves better video quality with the major drawback in the decoding delay for satisfying real-time requirements.

4 Experiment

The three scenarios, WLAN-only, 3G-only and integrated 3G/WLAN video streaming performance are compared. The experiments apply the proposed three-state Markov model, using the standard Akiyo sequence with the CIF format and the frame rate at 30 frames per second. PFGS is used to encode the video sequence, and each frame of the coded bitstream is sliced into 400 bits blocks. Extra stuffing bits are used for frames less than 400 bits. Four layers (one base-layer plus three enhancement layers) are transmitted over the WLAN hotspot and integrated 3G/WLAN experiments, and three layers are transmitted over the 3G experiment due to lower bandwidth capability. While the experiment is based on VBR stream with different channel capacity (WLAN and 3G), and under multipath delivery (3G/WLAN), the lost-pattern for WLAN, 3G and 3G/WLAN are independent to each other and should not be plotted under the same graph.

The parameters used for the three-state Markov chain is summarised in Table 1. The parameter chosen denotes the higher error prone behaviour on the WLAN network over the 3G network (P_{01} and P_{10}), as well as more frequent and longer handover state on WLAN over 3G (P_{12} and P_{21}). For the integrated 3G/WLAN simulation, since the base layer video is transmitted over the 3G network, P_{01} is lower than the scenario where all base and enhancement layers are transmitted over pure 3G network.

Table 1 Parameters for the three-state Markov chain model

	P_{01}	P_{10}	P_{12}	P_{21}
WLAN	0.01	0.60	0.30	0.30
3G	0.02	0.98	0.001	0.85
3G/WLAN: WLAN part	0.01	0.60	0.30	0.30
3G/WLAN: 3G part	0.005	0.98	0.001	0.85

The actual received video layers are shown in Figure 6. WLAN hotspot network is capable of providing a larger throughput than the 3G network, and therefore may be used to stream a high quality video. However, the relative higher error probability makes it error prone. 3G network, while stressed to transmit three video layers, increases the error probability and loss frames are also observed. Under the same condition, the integrated 3G/WLAN network experience less frame loss. Comparing Figure 6(a)–(c), we observe that 3G/WLAN system effectively removes the base-layer corruption from the WLAN. Comparing Figure 6(a)–(c), we observe that by offloading enhancement layer traffic from 3G to WLAN network, less base-layer corruptions are observed. The mean received video layers are 3.84 for WLAN, 2.93 for 3G and 3.90 for 3G/WLAN. While taking the drifting error into account, the actual decode-able video layers are 3.14 for WLAN, 2.44 for 3G and 3.30 for 3G/WLAN, as shown in Figure 7. With the decode-able video layers, the video can be reconstructed, and the decoded video quality is shown in Figure 8. We observed that 3G/WLAN outperforms WLAN by 2.32 dB on average, and outperforms 3G by 5.22 dB on average.

Figure 6 Received video layers (a) WLAN (mean = 3.84); (b) 3G (mean = 2.93); (c) 3G/WLAN (mean = 3.90)

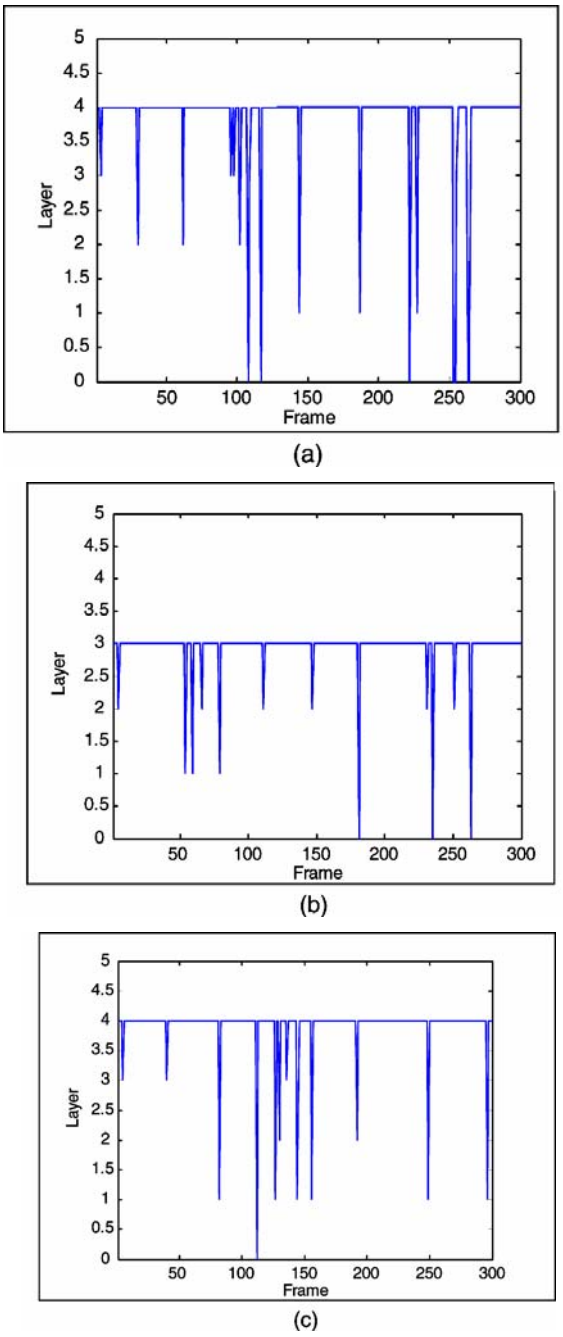

Figure 7 Decoded video layers accounting drifting error (a) WLAN (mean = 3.14); (b) 3G (mean = 2.44); (c) 3G/WLAN (mean = 3.30)

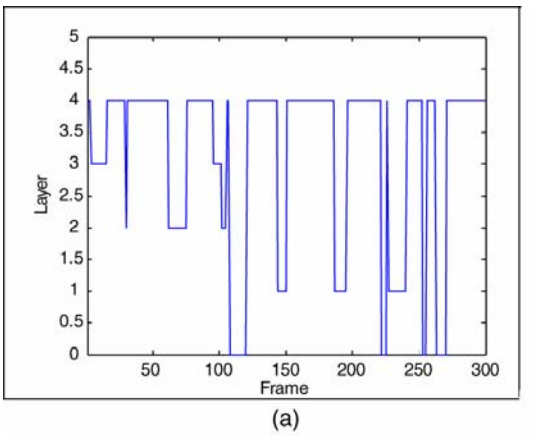

Figure 7 Decoded video layers accounting drifting error (a) WLAN (mean = 3.14); (b) 3G (mean = 2.44); (c) 3G/WLAN (mean = 3.30) (continued)

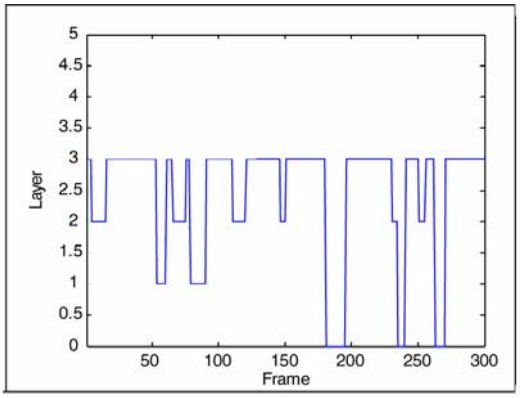

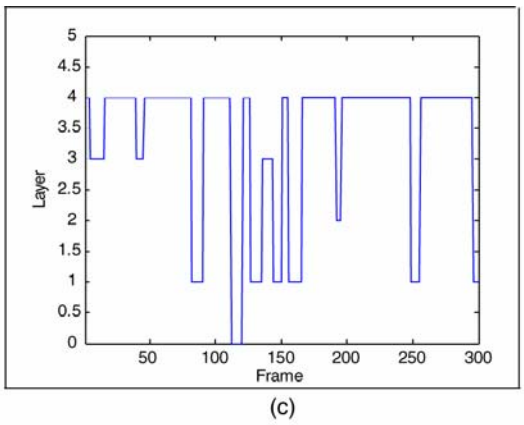

Figure 8 Decoded video quality in PSNR (a) WLAN (mean = 33.49 dB); (b) 3G (mean = 30.59 dB); (c) 3G/WLAN (mean = 35.81)

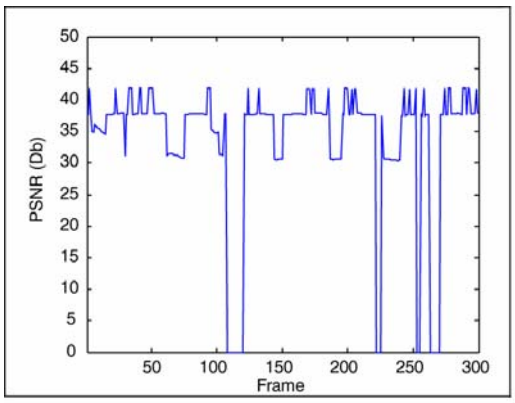

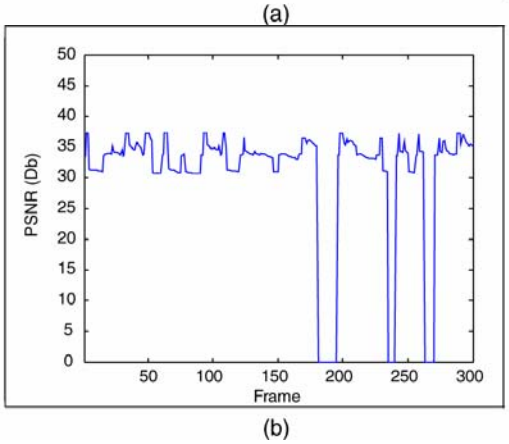

Figure 8 Decoded video quality in PSNR (a) WLAN (mean = 33.49 dB); (b) 3G (mean = 30.59 dB); (c) 3G/WLAN (mean = 35.81) (continued)

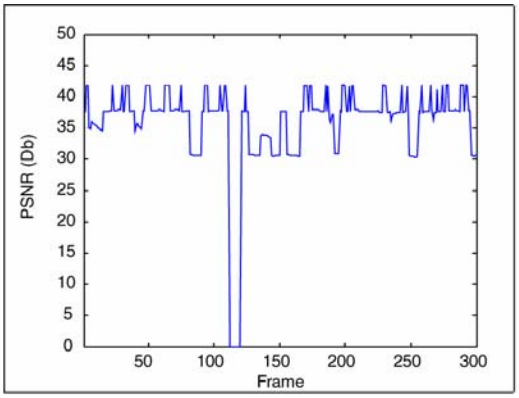

The same setup was used with an additional UEP channel coding. For simplicity, we apply AWGN as the channel error model with 3.5 dB Eb/*N*0, and the result is shown in Figure 9. Comparing Figures 6(c) and 9(a), we observe that most of the new frame loss behaviour is introduced in layers 3 and 4, while additional frame drop is observed for lower layers. This reflects the effectiveness of the UEP coding. As shown in Figure 9(c), the average video quality is slightly affected (down from 35.81 to 34.21 dB) with channel errors (Eb/*N*0 = 3.5 dB).

Figure 9 UEP with turbo code (a) received layers (mean = 3.81); (b) decoded layers (mean = 2.88); (c) decoded quality (mean = 34.21 dB)

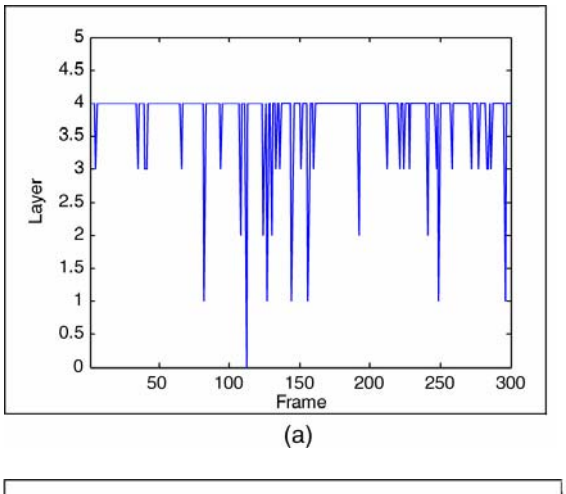

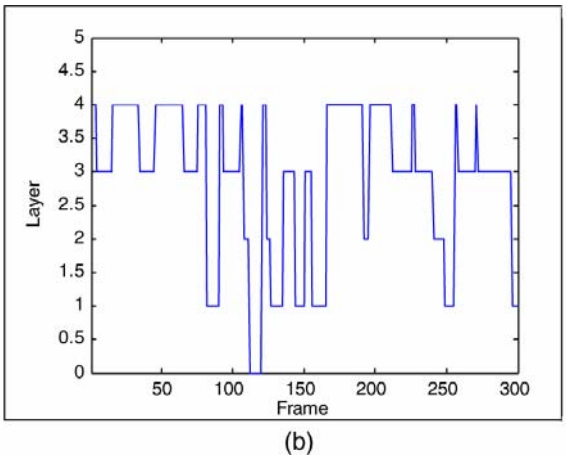

Figure 9 UEP with turbo code (a) received layers (mean = 3.81); (b) decoded layers (mean = 2.88); (c) decoded quality (mean = 34.21 dB) (continued)

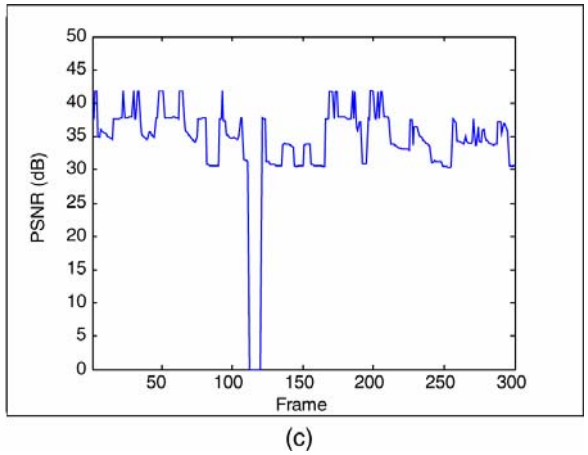

For the scenario where the base-layer was dropped in the integrated 3G/WLAN system, there is no data to reconstruct the lost frames. Instead of displaying blank video, intermediate frame are added using the cubic-spline extrapolation and interpolation techniques. In this experiment, the video frames 112–120 are missing. Different cubic-spline reference points are used and the results are shown in Figure 10. Figure 10(a) and (b) both use reference frames prior to the frame corruption, and we observe that increasing the number of reference frames does not necessarily improve the extrapolation quality, and in our experiment it is actually generating worst video quality. Figure 10(c) takes reference frames from both before and after the loss frames, and its performance clearly outperforms Figure 10(b). However, the drawback of bidirectional interpolation approach used in Figure 10(c) is the delay, as the client needs to receive the subsequent *I*-frame to generate the missing frames. Figures 11 and 12 show the actual video frames of Figure 10(b) and (c).

Figure 10 Frame recovery using cubic-spline extrapolation and interpolation (a) based on frame 108 to 111; (b) based on frame 110 to 111; (c) based on frame 110, 111 and 121, 122

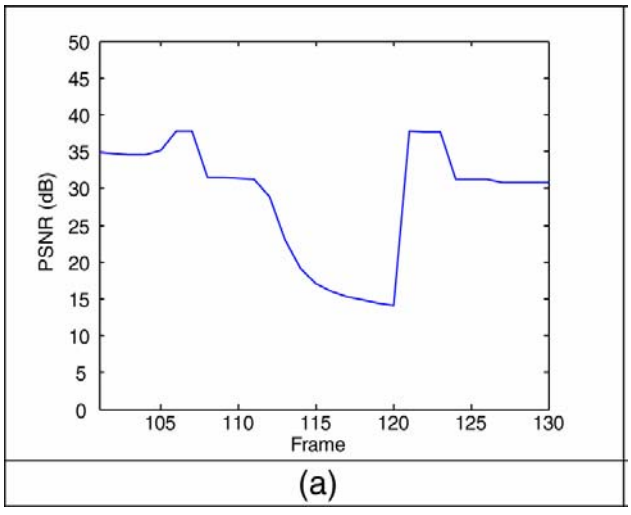

Figure 10 Frame recovery using cubic-spline extrapolation and interpolation (a) based on frame 108 to 111; (b) based on frame 110 to 111; (c) based on frame 110, 111 and 121, 122 (continued)

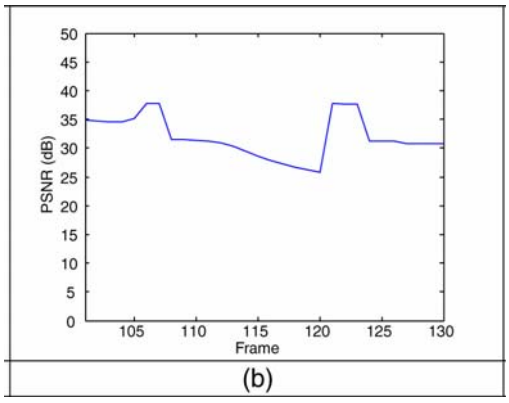

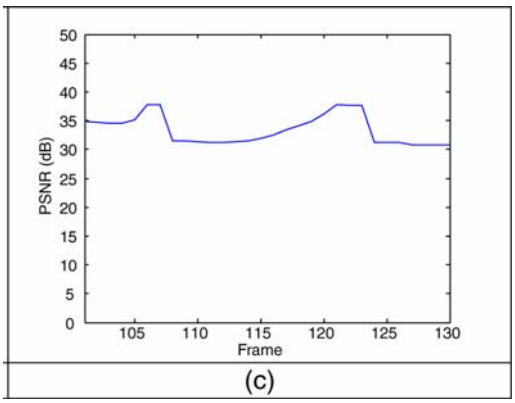

Figure 11 Reconstructed video frames Figure 10(b)

Figure 12 Reconstructed video frames of Figure 10(c)

5 Conclusions

In this paper, we presented the integrated 3G/WLAN video streaming system. By utilising the high bandwidth in WLAN hotspot network to stream enhancement layers, and utilising the readily-developed 3G network to stream base layer, a lower frame dropout was observed according to our simulation using a three-state Markov chain model.

For errors introduced by signal fading and noise interference, a UEP channel codec based on Turbo code was integrated in the proposed system. Our simulation results show an increased frame dropout rate due to channel errors are limited to the top video layer, reflecting the effectiveness of the UEP to protect sensitive base layer information.

Cubic-spline extrapolation and interpolation techniques were proposed to reconstruct lost video frames. We observed that the bi-directional interpolation outperforms uni-directional extrapolation, with the tradeoff in the decoding delay.

From our observation, we conclude that the integrated 3G/WLAN system for video streaming yields superior video qualities over 3G-only and WLAN-only solutions.

Acknowledgements

The authors would like to acknowledge Microsoft Research Asia for providing the PFGS source code for the simulation. This project is supported in part by Canada Research Chair Program and Canada Foundation for Innovation. This paper is based on the work when the author was affiliated with the University of Sydney, Australia.

References

Berrou, C., Glavieux, A. and Thitimajshima, P. (1993) 'Near shannon limit error correcting coding and decoding: turbo-codes', *Proceedings of International conference on Communication*, Geneva, Switzerland, May, pp.1064–1070.

Karim, H.A., Bister, M. and Siddiqi, M.U. (2003) 'Low rate video frame interpolation – challenges and solution', *Proceedings of International Conference on Acoustics, Speech and Signal Processing*, Vol. 3, pp.117–120.

Lehmann, T., Gonner, C. and Spitzer, K. (1999) 'Survey: interpolation methods in medical image processing', *IEEE Transactions on Medical Imaging*, Vol. 18, No. 11, pp.1049–1075.

Li, W. (2001) 'Overview of fine granularity scalability in MPEG-4 video standard', *IEEE Transactions on Circuits and Systems for Video Technology*, Vol. 11, pp.301–317.

Mao, S., Lin, S., Panwar, S., Wang, Y. and Celebi, E. (2003) 'Video transport over ad hoc networks: multistream coding with multipath transport', *IEEE Journal on Selected Areas in Communications*, Vol. 21, No. 10, pp.1721–1737.

Ostermann, J., Bormans, J., List, P., Marpe, D., Narroschke, M., Pereira, F., Stockhammer, T. and Wedi, T. (2004) 'Video coding with H.264/AVC: tools, performance, and complexity', *IEEE Circuits and Systems Magazine*, Vol. 4, No. 1, pp.7–28.

Stockhammer, T., Hannuksela, M. and Wiegand, T. (2003) 'H.264/AVC in wireless environments', *IEEE Transactions on Circuits and Systems for Video Technology, Special Issue on the H.264/AVC Standard*, Vol. 13, No. 7, pp.657–673.

Stockhammer, T., Jenkac, T. and Kuhn, G. (2004) 'Streaming video over variable bit-rate wireless channels', *IEEE Transactions for Multimedia (Special Issue on Streaming Media*, April, pp.268–277.

Stockhammer, T., Jenkac, H. and Weiß, C. (2002) 'Error protection and feedback strategies for wireless progressive video transmission', *IEEE Transactions on Circuits and Systems for Video Technology, Special Issue on Wireless Video*, Vol. 12, No. 6, pp.465–482.

Wiegand, T., Sullivan, G.J., Bjontegaard, G. and Luthra, A. (2003) 'Overview of the H.264/AVC video coding standard', *IEEE Transactions on Circuits and Systems for Video Technology*, Vol. 13, No. 7, pp.560–576.

Wu, D., Hou, Y.T. and Zhang, Y-Q. (2001a) 'Scalable video coding and transport over broad-band wireless networks', *Proceedings of IEEE*, Vol. 89, No. 1, pp.6–20.

Wu, D., Hou, Y.T., Zhu, W., Zhang, Y-Q. and Peha, J.M. (2001b) 'Streaming video over the internet: approaches and directions', *IEEE Transaction on Circuits and Systems for Video Technology*, Vol. 11, No. 3, pp.282–300.

Wu, F., Li, S. and Zhang, Y-Q. (2001c) 'A framework for efficient progressive fine granularity scalable video coding', *IEEE Transactions on Circuits and Systems for Video Technology*, Vol. 11, pp.332–344.

Yang, F., Zhang, Q., Zhu, W. and Zhang, Y-Q. (2004) 'Bit allocation for scalable video streaming over mobile wireless internet', *Proceedings of IEEE INFOCOM 2004*.

Yee, J.R. and Weldon, E.J. (1995) 'Evaluation of the performance of error-correcting codes on a gilbert channel', *IEEE Transactions on Communication*, Vol. 43, pp.2316–2323.

Zhang, T. and Xu, Y. (1999) 'Unequal packet loss protection for layered video transmission', *IEEE Transactions on. Broadcasting*, Vol. 45, pp.243–252.

Appendix

Steady state analysis

From Equation (2), the steady state probabilities P satisfies $P \times P_s = P_s$. To simplify P, the loopback probabilities $\{P_{00}, P_{11}, P_{22}\}$ can be expressed in terms of the transition probabilities, $\{P_{01}, P_{10}, P_{12}, P_{21}\}$, as shown in Equations (A1)–(A3).

$$P_{00} = 1 - P_{01} \tag{A1}$$

$$P_{11} = 1 - P_{10} - P_{12} \tag{A2}$$

$$P_{22} = 1 - P_{21} \tag{A3}$$

As illustrated in Equation (A4), row 2 represents a linear combination of rows 1 and 3.

$$P = \begin{bmatrix} 1-P_{01} & P_{10} & 0 \\ P_{01} & 1-P_{12}-P_{10} & P_{21} \\ 0 & P_{12} & 1-P_{21} \end{bmatrix} \tag{A4}$$

With the three-state Markov chain, the model should satisfy Equation (A5). Therefore, the steady state analysis may be rearranged in Equation (A6).

$$P_{S0} + P_{S1} + P_{S2} = 1 \tag{A5}$$

$$\begin{bmatrix} P_{00}-1 & P_{10} & 0 \\ 0 & P_{12} & P_{22}-1 \\ 1 & 1 & 1 \end{bmatrix} \begin{bmatrix} P_{S0} \\ P_{S1} \\ P_{S2} \end{bmatrix} = \begin{bmatrix} 0 \\ 0 \\ 1 \end{bmatrix} \tag{A6}$$

Solving Equation (A6) and the steady state probability of Good, Bad and Handover states yields Equation (A7).

$$\begin{bmatrix} P_{S0} \\ P_{S1} \\ P_{S2} \end{bmatrix} = A \begin{bmatrix} P_{10}(1-P_{22}) \\ (1-P_{00})(1-P_{22}) \\ (1-P_{00})P_{12} \end{bmatrix} \tag{A7}$$

where

$$A = \frac{1}{-P_{00}P_{12} + P_{00}P_{22} - P_{00} + P_{12} - P_{22} + 1 + P_{10} - P_{10}P_{22}}$$

Finally, substituting the loopback state probability with transition probabilities from (A1) to (A3), the steady state probabilities in (A7) may be simplified to (A8).

$$\begin{bmatrix} P_{S0} \\ P_{S1} \\ P_{S2} \end{bmatrix} = \frac{1}{P_{01}P_{12} + P_{01}P_{21} + P_{10}P_{21}} \begin{bmatrix} P_{10} & P_{21} \\ P_{01} & P_{21} \\ P_{01} & P_{12} \end{bmatrix} \tag{A8}$$